Impact of feeding position on the performance and characteristics of small wearable on-ground antennas

Progress In Electromagnetics Research C, Vol. 57, 53–60, 2015

Impact of Feeding Location on On-Body Performance of Small On-Ground Antennas

Tommi Tuovinen[1, *], Markus Berg[1], and William G. Whittow[2]

Abstract—In this paper, three commonly used on-ground antenna types (loop, monopole and planar inverted-F antenna) are compared in the scope of wireless body area networks (WBAN) for on-body communications at 2.45 GHz. The bandwidth of the antennas can be enhanced by placing them towards the edge or the corner of the small ground plane ($25 \times 35\,\mathrm{mm}^2$) which has, as a consequence, detrimental effects on radiation characteristics that motivates the examination of the impact of feeding location for on-body propagation in detail. The present study quantifies the trade-off between on-body efficiency, the gain in the direction tangential to the surface, applicability to launch creeping waves and bandwidth potential of the different antenna types with various feeding locations. The simulated channel gain $|S_{21}|$ around tissue-equivalent numerical phantoms is compared to an analytical WBAN path loss model.

1. INTRODUCTION

On-body antennas have a notable impact on the system performance of IEEE802.15.6 [1] applications for a wireless body area network (WBAN) [2], which require low power devices (or sensor nodes). The antenna presents a significant challenge in the miniaturization of wearable sensor nodes because of the achievable radiation performance is directly linked to the size of an antenna. The advancement in conducting textiles, has allowed traditional rigid antennas [3, 4] to be considered as a new generation of wearable antennas.

One of the often discussed challenges in the field is efficient propagation along a body surface, especially to the back side of a user wearing a sensor on the torso. The fundamental problem is to overcome the high channel loss that is the combination of free space and tissue losses. With specific relevance to this paper, researchers have carried out studies related to the creeping wave theory (CWT) [5]. One of the main conclusions is that the on-body propagation is superior with a polarization normal to the body surface as opposed to tangential to the body [6, 7]. The latter is typical characteristic of wearable antennas that are typically planar [8, 9]. By achieving the dominant normal polarization to the body, significantly improved path gain on a link can be achieved, which results in lower power consumption or higher node-to-node distances. Recent studies have also been examined propagation around a head [10, 11] or along a body surface [12, 13].

The change in the operation of an antenna, caused by a body, in relation with free space can be explained by using the perturbation theory: due to impact of tissues, the resonant frequency shifts downwards and the interaction with a body is mainly via the electric field. Moreover, in the proximity of a body, the shape of a pattern changes and the radiation efficiency reduces due to absorption in the tissues [14]. The human body effect varies between the type of antenna and the size of the ground plane.

To the authors' knowledge, different antenna types have not been comprehensively compared for the WBAN context and channel path gain performance is not compared with the available channel model.

Received 6 February 2015, Accepted 15 April 2015, Scheduled 20 April 2015

* Corresponding author: Tommi Tuovinen (tommi.tuovinen@ee.oulu.fi).

[1] Centre for Wireless Communications (CWC), P.O.B. 4500, FI-90014, University of Oulu, Finland. [2] School of Electronic, Electrical and Systems Engineering, LE11 3TU, Loughborough University, UK.

This paper is restricted to consider the propagation around a body in the situation that both antennas are at the same cross-section of the body, in which case the CWT is theoretically valid [6]. For the examination of the propagation of surface waves in body's longitudinal directions, Norton surface wave models [15] are valid, which are beyond the scope. In the present paper, we compare the performance of various on-ground antenna types at 2.45 GHz operation [16] against the first deterministic analytical WBAN model [6], which was derived according to the diffraction theory and takes into account body morphology and tissue characteristics. The impact of the on-ground feeding location for various antenna characteristics is also examined.

2. ANTENNAS AND SIMULATION SETUP

This section explains the chosen antenna types.

A PIFA or a patch is known to have promising characteristics for off-body communications as the maximum gain is in the normal direction to the radiator plate and its' polarization has both normal and tangential components. A monopole antenna has suitable characteristics for on-body communications because of the tangential maximum gain and a dominant normal polarization. In general, the size of the monopole is unpractical for sensor nodes, but there are possibilities for the miniaturization, such as meandering or dielectric loading (with high-ε_r substrate). Typically, a loop antenna is not as widely accepted as a monopole or a patch for mobile communications, e.g., due to the complexity to generate multi-resonance operation. Nevertheless, it is commonly used, e.g., when a symmetrical radiator pattern with respect to a feed location is required. It is of interest to compare the on-body performance of the loop with the widely used PIFA and monopole antennas. Due to these reasons, throughout the paper, three on-ground antenna types are investigated: loop, meandered monopole and PIFA. In addition, the discone is considered as a reference antenna with a pure normal polarization to the body's surface.

To allow a fair comparison of antenna types, a starting point for the on-body optimisation procedure is with the antennas fed in the middle of a ground plane introduced in [17]. The middle of a ground is far from the best feeding alignment in terms of bandwidth (BW). In order to achieve the widest bandwidth, the most suitable feeding position is in the corner of a rectangular ground plane [18, 19]. In free space conditions, allowing the antenna to extend beyond the ground plane (increasing the antenna ground clearance) further improves the radiation efficiency [20].

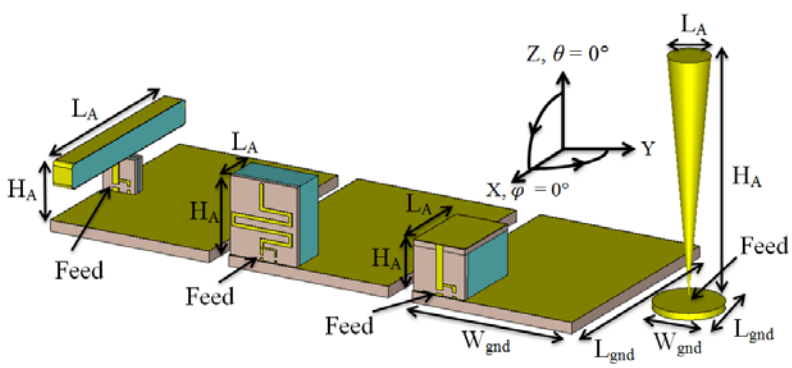

Figure 1. Oblique views to show feeding positions and to indicate the size of the antennas to cover the spectrum at 2400–2483 MHz: on-ground loop, monopole and PIFA, and reference discone. A blue support material is modelled by $\varepsilon_r \approx 1$ and $\tan\delta < 0.002$ below 11 GHz, the dielectric below of a ground is made of FR4 (grey) and the conductive parts are of copper (yellow).

In this study, the antenna feed location is optimised in terms of the impedance bandwidth by considering the BW potential (-10 dB symmetric BW at various feeding locations on a small ground plane). Fig. 1 shows the geometry of BW-optimised antennas ensuring the entire radiator is completely above the ground. The dimensions of the antennas are in Table 1. The circumference of loop, the length of the meandered monopole and the length of the PIFA element are $\sim 0.6\lambda$, $\sim 0.35\lambda$ and $\sim 0.15\lambda$, respectively. The size of a flat reduced ground plane ($25 \times 35\,\text{mm}^2$) on top of a 1.6 mm thick

Table 1. Dimensions of the 2.45 GHz antennas in Fig. 1.

Antennas	Antenna dimensions (mm)			
	W_{gnd}	L_{gnd}	H_A	L_A
Loop on-ground	35	25	9.2	30.6
Monopole on-ground	35	25	11.5	1.6
PIFA on-ground	35	25	8.0	11.6
Reference: Discone	10	10	34.9	6.0

FR4, was chosen based on the size of a practical, realistic on-body sensor nodes. A shunt inductor is placed on the shorting line next to the feed position to match each antenna. The values of the inductors are 20 nH, 2 nH and 0.9 nH for the loop, monopole and PIFA, respectively.

Simulations are used in this paper because the effects of changing the individual parameters to be isolated while the other metrics remain identical. In addition, simulations neglect the impact of well-known cable effects in the experiments with a small ground plane that changes the antenna impedance and causes the feeding cable to radiate. Note, in real WBAN applications the measurement cables are not present. Furthermore, measurements with phantoms are prohibitively expensive and include an unrealistic plastic shell while measurements on real volunteers are very sensitive to the shape of the body, the posture, the position of the arms, clothing and also respiration. These sources of uncertainty can be avoided in the simulations. An analytical model is used as a comparison with the simulated results.

In this study, propagation around a human body surface is approximated by using lossy cylinders. In [6], it was shown that cylinders can be used to model different body parts. The dielectric properties of cylinders are defined as skin tissue ($\varepsilon_r = 38.1$ and $\sigma = 1.4$ S/m). The body cylinder is 600 mm long in the X axis and has a diameter of 150 mm unless specifically stated otherwise. Simulations are carried out by using Computer Simulation Technology (CST) software [21].

3. ON-BODY PERFORMANCE OF THE STUDIED ANTENNAS

Figure 2 depicts reflection coefficients and total efficiencies for the studied antennas. In comparison with the antennas located centrally on the ground planes in [17], the achieved advantage of the optimisation of a feed location in terms of bandwidth is notable: the −10 dB impedance matching of loop, monopole and PIFA is increased by 44%, 100% and 76%, respectively.

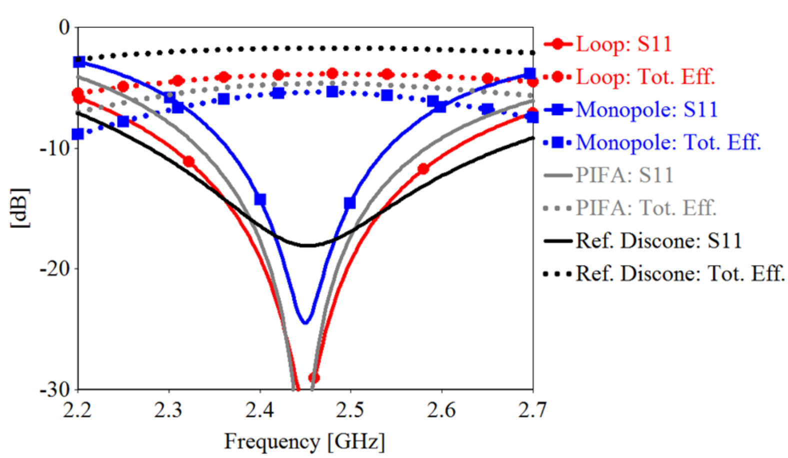

Figure 2. Reflection coefficient and total antenna efficiency for the BW-optimised antennas on the body.

As expected, by optimising the feeding to the best position based on the BW potential, i.e., close to the edge of the ground plane, results in a drop of efficiency. The BW-optimised loop, monopole and PIFA accomplish only 83%, 63% and 66% of the efficiency achievable with the feeding in the middle of a ground plane in [17]. The reason is due to the fact that the BW-optimised feeding positions tend to have higher absorption of the antenna's reactive near-field in tissues due to the increased ground clearance. The fractional bandwidth and total antenna efficiency are summarised in Table 2.

Table 2. On-body performance of the antennas.

Antennas	**Fractional Bandwidth**	**Total Efficiency at 2.45 GHz**
Loop on-ground	13%	41%
Monopole on-ground	7%	29%
PIFA on-ground	10%	34%

The impact of the BW-optimization on channel path gain performance is evaluated in Fig. 3. In simulations, one antenna is rotated in steps of 7.5° (i.e., a rotation angle in the graphs) around the 200 mm cylinder while the other antenna stays stationary. The on-ground configurations are placed on contact with the phantom whereas the reference discone is operated at $\lambda_0/4$ on the phantom for matching purposes. The solid line in Fig. 3 is the analytical WBAN model [6], which can be expressed by

$$G=\frac{P_{\mathrm{RX}}}{P_{\mathrm{TX}}}=\frac{c^{10/6}\pi^{4/3}}{4\pi^2\left|1-0188e^{-j\pi/3}\right|^2}G_{\mathrm{TX}}G_{\mathrm{RX}}\frac{1}{d}\frac{1}{f^{10/6}}\frac{1}{a^{2/3}}\times\left|\left[e^{-\alpha d}e^{-jkd}+e^{-\alpha(p-d)}e^{-jk(p-d)}\right]^2\right|, \quad (1)$$

$$\text{and}\quad \alpha_{Np/m}=\frac{\pi^{1/3}\left|1-0188e^{-j\pi/3}\right|\cos\pi/6}{\lambda^{1/3}a^{2/3}}, \quad (2)$$

where G and P are gain and power of the antenna, k is linked to the impedance of the body surface, α is the attenuation factor $[Np/m]$. All the factors are explained in the original paper [6].

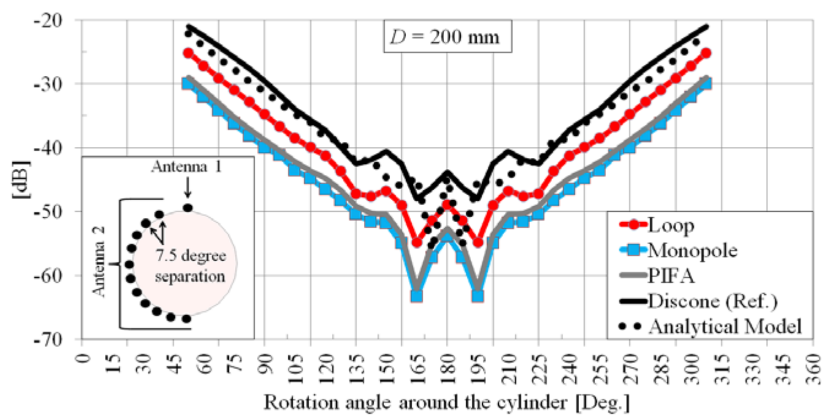

Figure 3. Channel path gain performance S_{21} for the studied antennas: loop, monopole, PIFA, and reference discone in the proximity of a 200 mm cylinder for the BW-optimised antennas.

The middle-fed on-ground configurations in [17] proved that the antenna type has a very small impact on the achievable path gain and the channel deviation stays minor with respect to the available path loss model [6].

The results of this study indicate a reduced path gain with the analytical model due to the BW-optimisation according to the feeding location: the path gain with respect to the analytical model is reduced, especially for the loop and monopole antennas, when the feeding position is located closer to the edge of a ground plane. As each studied antenna type satisfies reflection coefficient $S_{11}\leq-20$ dB, the impact of matching to cause the path gain reduction can be ignored. Moreover, since the antennas maintain the dominant normal polarization with respect to the body surface, it is understood that the residual factor explaining the reduced path gain is because of following factors: the unfavourable variation of a pattern shape (and the reduced efficiency [4]) and the diminished capability of the antenna to generate purely normally-polarized field components. The results have similar trends with different sizes of cylinders except with the magnitudes in S_{21} changed.

4. IMPACT OF FEEDING LOCATION ON ON-BODY PERFORMANCE

In this section, the impact of on-ground feeding position on performance is demonstrated in terms of efficiency, BW potential (calculated in CST by using -10 dB symmetrical bandwidth with ideal two component matching) and realized gain in different planes. The aim is to evaluate the trade-off between the parameters under discussion as a function of the feeding location. In this part, ground clearances are used (where the radiator extends beyond the ground plane) in order to position the feeding close to the edge of the ground.

Figure 4 compares the performance in terms of efficiencies and BW potential for the on-ground configurations. For the considered feed positions the entire antenna structure including a port and a shunt inductor is moved from the edge to the middle of a ground plane in steps of 1 mm. The distance is measured from the feeding port to the edge of the ground. The performance behaviour is in general similar between the antenna types. The widest BW potential is acquired if the feeding is as close as possible to the edge of the ground plane. The loop antenna shows the most promising BW potential varying through the values of 368–198 MHz, while the variation of 147–89 MHz and 266–138 MHz are observed for the monopole and PIFA, respectively. The widest impedance bandwidth of

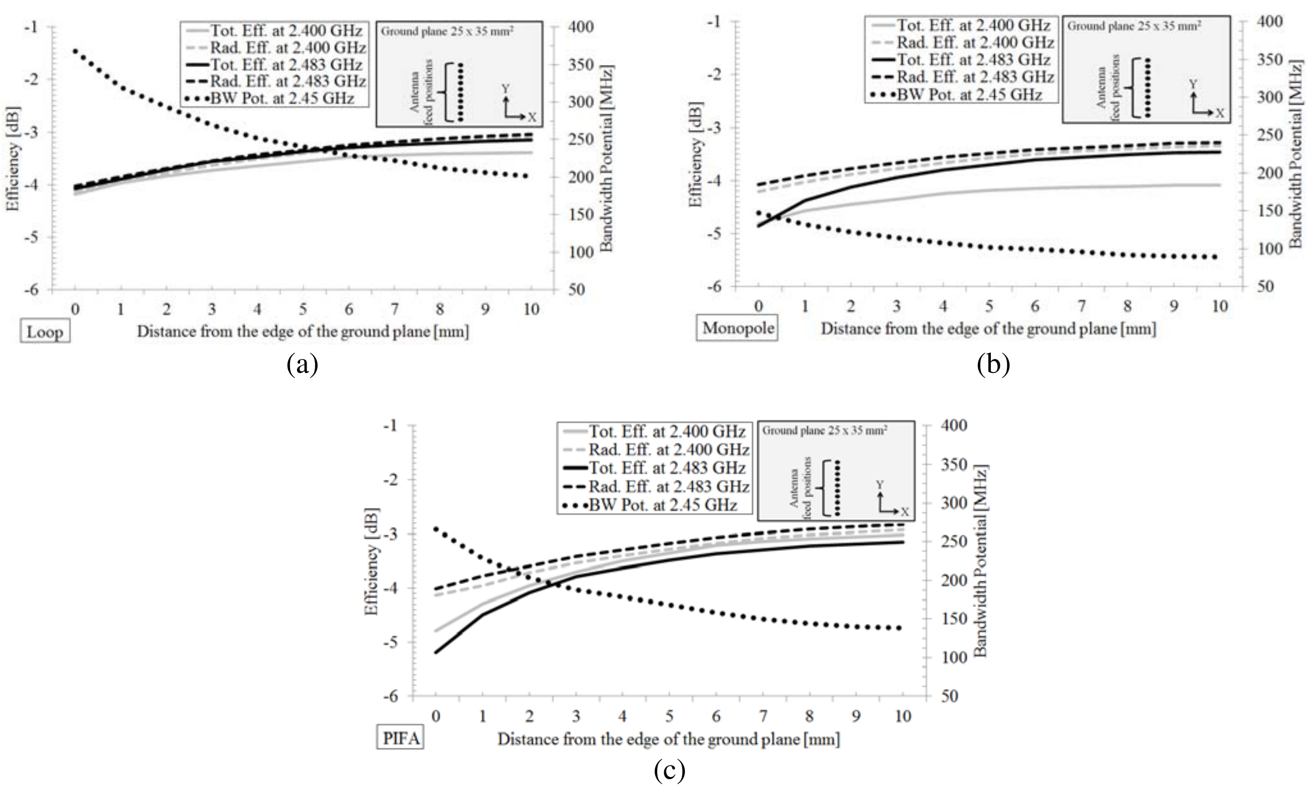

Figure 4. Total antenna and radiation efficiencies [dB] presented together with BW potential [MHz] as a function of the antenna feed point distance from the edge of the ground plane for (a) loop, (b) monopole, and (c) PIFA.

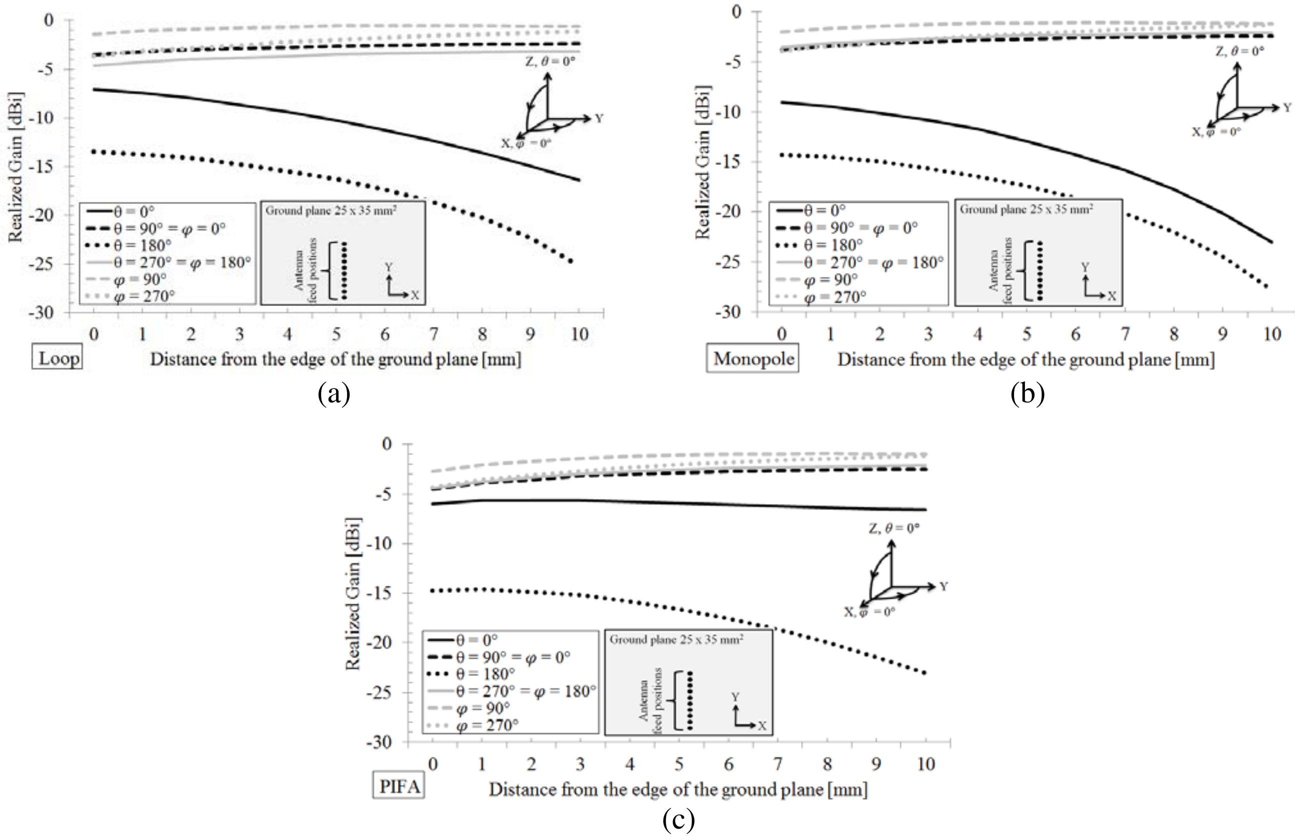

Figure 5. Realized gain [dBi] as a function of the antenna feed position distance from the edge of the ground for (a) loop, (b) monopole and (c) PIFA.

the loop is due to having the largest volume and hence the smallest Q factor, as the connection is with $Q = 1/(kr)^3 \approx 1/\mathrm{FBW} = f_0/\Delta f$, where r is the radius of the Radian sphere, FBW is the fractional bandwidth and f is the frequency. While moving the feed to the middle of a ground results in narrower bandwidth and efficiency will be improved. The improvement of total antenna efficiency vary within the studied range (2.400/2.483 MHz) are 0.8/0.9 dB for the loop, 0.7/1.4 dB for the monopole, and 1.8/2.1 dB for the PIFA.

Figure 5 depicts the behaviour of realized gain in the azimuthal and elevation planes as a function of the feeding location. Moving the feed towards the middle of the ground plane clearly improves the pattern gain performance in the tangential direction, i.e., in the xy-plane with respect to a body: almost ideal omnidirectional radiation is observed in the tangential plane with respect to the body surface for the feeding location in the middle of a ground. The increase in the tangential gain with the distance from the centre of the ground plane is the fastest in the direction of the feeding, i.e., 270° (the grey dashed line) in the studied setup. Moreover, by placing the antenna radiators near the edge of the ground plane, loop and monopole alter the classic doughnut shape pattern (in the xz- and zy-planes) and direct more gain towards the normal direction to the body (xz- and zy-planes), which is not propitious for the on-body antenna that should minimise off-body radiation. It should be noted that the pattern shape is able to show the absolute gain in the tangential direction, despite the pattern gain plots do not take into account the impact of body's surface waves that starts to travel around a body shape, and is dependent on the antenna polarization. In particular, the tangential gain can be suggestive, but does not tell the truth of the achievable channel performance around a body shape. In order to indicate the parameter showing the greatest variation in the performance, i.e., channel path gain, another antenna must be used as a probe to capture the gain performance in the positions of the interest to verify the antenna on-body capability, for instance, with the method as was implemented in Fig. 3.

5. CONCLUSION

In the present paper, the impact of the antenna feeding location on the on-body performance has been studied. The research hypothesis was related to the trade-off between the impedance bandwidth and desirable on-body characteristics, based on the feed point position. By placing the antennas towards the edge of the ground plane, the BW was increased but the efficiency, pattern shape and channel path gain were observed to decrease. In general, simulations showed good agreement with the analytical model. Investigations confirmed that, although various types of antenna have been studied, the dominant field polarization is normal with the body surface (in the z-direction) due to the impact of the ground plane. From a small WBAN sensor node perspective, in order to maximise channel path gain performance, the most desirable feeding location is in the middle of a ground plane, if the antenna bandwidth in a wearable device can be compromised.

ACKNOWLEDGMENT

This work was supported in part by the Academy of Finland and Centre for Wireless Communications.

REFERENCES

1. "IEEE standard for local and metropolitan area networks," IEEE 802.15.6-2012 — Part 15.6: Wireless Body Area Networks, 2012.
2. Hall, P. S. and Y. Hao, *Antennas and Propagation for Body-Centric Wireless Communications*, 2nd edition, Artech House, Norwood, 2012.
3. Alves, T., B. Poussot, and J.-M. Laheurte, "PIFA-top-loaded-monopole antenna with diversity features for WBAN applications," *IEEE Antennas Wirel. Propag. Lett.*, Vol. 10, 693–696, 2011.
4. Conway, G. A. and W. G. Scanlon, "Antennas for over-body-surface communication at 2.45 GHz," *IEEE Trans. Antennas Propag.*, Vol. 57, No. 4, 844–855, 2009.
5. Paknys, R. and N. Wang, "Creeping wave propagation constants and modal impedance for a dielectric coated cylinder," *IEEE Trans. Antennas Propag.*, Vol. 34, No. 5, 674–680, 1986.
6. Alves, T., B. Poussot, and J.-M. Laheurte, "Analytical propagation modeling of BAN channels based on the creeping-wave theory," *IEEE Trans. Antennas Propag.*, Vol. 57, No. 4, 1269–1274, 2011.
7. Fort, A., F. Keshmiri, G. R. Crusats, C. Craeye, and C. Oestges, "A body area propagation model derived from fundamental principles: Analytical analysis and comparison with measurements," *IEEE Trans. Antennas Propag.*, Vol. 58, No. 2, 503–514, 2010.
8. Lin, C. H., K. Saito, M. Takahashi, and K. Ito, "A compact planar inverted-F antenna for 2.45 GHz on-body communications," *IEEE Trans. Antennas Propag.*, Vol. 60, No. 9, 4422–4426, 2012.
9. Soh, P. J., G. A. E. Vandenbosch, S. L. Ooi, and N. H. M. Rais, "Design of a broadband all-textile slotted PIFA," *IEEE Trans. Antennas Propag.*, Vol. 60, No. 1, 379–384, 2012.
10. Kvist, S. H., J. Thaysen, and K. J. Jakobsen, "Polarization of unbalanced antennas for ear-to-ear on-body communications at 2.45 GHz," *Proc. 7th Loughborough Antennas Propag. Conf. (LAPC)*, 1–4, United Kingdom, Nov. 2011.
11. Khandra, R. and A. J. Johansson, "Influence on the ear-to ear link loss from heterogeneous propagation channel," *Proc. 5th Europ. Conf. Antennas Propag. (EuCAP)*, 1612–1615, Rome, Italy, Apr. 2014.
12. Grimm, M. and D. Manteuffel, "Far field modeling of body worn antennas by the superposition of equivalent electric sources," *Proc. 8th Europ. Conf. Antennas Propag.*, 1754–1755, Hague, Netherlands, Apr. 2014.
13. Tuovinen, T., M. Berg, and E. Salonen, "The effect of antenna pattern and polarization for launching creeping waves on a skin surface," *Proc. Europ. Conf. Antennas Propag. (EuCAP)*, 1960–1963, Netherlands, Apr. 2014.

14. Tuovinen, T., M. Berg, and E. Salonen, "Antenna close to tissue: avoiding radiation pattern minima with anisotropic substrate," *IEEE Antennas Wireless Propag. Lett.*, Vol. 13, 1680–1683, 2014.
15. Grimm, M. and D. Manteuffel, "Norton surfaces waves in the scope of body area networks," *IEEE Trans. Antennas Propag.*, Vol. 62, No. 5, 2616–2623, 2014.
16. Bluetooth low energy regulatory aspects, bluetooth SIG regulatory committee, V10r00, 2011.
17. Tuovinen, T., M. Berg, W. G. Whittow, and E. Salonen, "Performance of WBAN on-ground antenna type with relation to analytical path loss model," *Proc. of 10th Loughborough Antennas Propag. Conf. (LAPC)*, UK, 2014.
18. Ilvonen, J., O. Kivekäs, J. Holopainen, R. Valkonen, K. Rasilainen, and P. Vainikainen, "Mobile terminal antenna performance with the user's hand: Effect of antenna dimensioning and location," *IEEE Antennas Wirel. Propag. Lett.*, Vol. 10, 772–775, 2011.
19. Vainikainen, P., J. Ollikainen, O. Kivekäs, and I. Kelander, "Resonator-based analysis of the combination of mobile handset antenna and chassis," *IEEE Trans. Antennas Propag.*, Vol. 50, No. 10, 1433–1444, 2002.
20. Krogerus, J., J. Toivanen, C. Icheln, and P. Vainikainen, "Effect of the human body on total radiated power and the 3-D radiation pattern of mobile handsets," *IEEE Trans. Instrum. Meas.*, Vol. 56, No. 6, 2375–2385, 2007.
21. Computer Simulation Technology Microwave Studio Software, Online Available: http://www.-cst.com.